



# Wideband Microstrip Array Antenna Using Defected Ground and Microstrip Structure for Monopulse Secondary Surveillance Radar Application

H. Bambang Bagus<sup>(✉)</sup>, Nyaris Pambudiyatno, Yuyun Suprpto, Iga Ayu Mas Oka, and Fiqqih Faizah

Politeknik Penerbangan Surabaya, Surabaya, Indonesia  
bambangfarzardy@gmail.com

**Abstract.** The wideband microstrip antenna is a development of the purpose of this study is to design a wideband antenna at a frequency of 1030 MHz–1090 MHz which will be applied to the Monopulse Secondary Surveillance Radar (MSSR) antenna. The study uses a single microstrip antenna using the DGS (Defected Ground Structure) method and the DMS (Defected Microstrip Structure) method, which can increase the antenna bandwidth. From the results of the element simulation, adding the DGS (Defected Ground Structure), and DMS (Defected Microstrip Structure) structures to the single antenna obtained a result of 2.83 dB.

**Keywords:** Antenna microstrip · Wideband · DGS (Defected Ground Structure) · DMS (Defected Microstrip Structure)

## 1 Introduction

Microstrip antennas are one of the various types of antennas whose development is very rapid. Microstrip antennas are an option because they have a lot of advantages such as lighter weight, practicality, small dimensions, and easy fabrication. Because of this advantage, microstrip antennas have been applied to modern telecommunications and surveillance equipment [1–6].

Monopulse Secondary Surveillance Radar (MSSR) is a tool to actively detect and find out the position and data of targets around it, where the aircraft is active if it receives a secondary radar RF signal beam. This radar beam is in the form of mode pulses, the aircraft installed with a transponder will receive these pulses and will answer in the form of code pulses to the radar receiving system. The MSSR Radar Station located below (Ground Station SSR) consists of Transmitter (Tx), Receiver (Rx), Processing or Video Extractor, Coder, and Monitor / Plane Position Indicator. The transmitter works at a carrier frequency of 1030 MHz modulated by Mode A and Mode C signals. Where this “interrogate signal” is modulated with “mode A”, it means that the transmitter or interrogator sends an inquiry about aircraft identification, and whenever the interrogator sends mode C it sends a signal question about the altitude of the aircraft. Mode A or mode

C is sent by the interrogator interlacing (alternately) The receiver receives an answer signal from the transponder of the aircraft with a frequency of 1090 MHz. When the interrogator sends mode A which is modulated with a carrier frequency of 1030 MHz, the transponder on the plane will receive this signal and will be sent back by the transponder (reply signal) in the form of a code signal and modulated with a carrier transponder signal of 1090 MHz, This code signal will be processed in the Video Extractor section and so on displayed on the monitor screen in the form of aircraft identification, as well as if the interrogator sends mode C, the information displayed on the monitor screen is "aircraft altitude". MSSR radar can detect the azimuth (coordinates) of the aircraft, the distance of the aircraft to the MSSR Station, and the speed of the aircraft, in addition to the identification and altitude of the aircraft [7–10].

Antennas are one of the most important components in the Monopulse Secondary Surveillance Radar (MSSR) communication system. The antenna serves as a transmitter and receiver of electromagnetic waves. Microstrip antennas are currently widely used in the world of telecommunications because of their practical shape, lightweight, and ease to plan and manufacture.

Microstrip antennas have several disadvantages including narrow bandwidth and low gain therefore some modifications are used as well as better applied at high frequencies. In the measurement process, it is often difficult to produce parameters due to the lack of equipment in measurements such as VNA, high-frequency analyzer spectrum, high-frequency counter as well as a room free from electromagnetic wave currents from various electronic equipment. In its development, the telecommunications and surveillance sectors are expected to be able to adapt to the needs and developments of technology 4.0.

To increase the efficiency, directivity, bandwidth, and gain of the antenna. This is because the single element has the characteristics of a large beam angle, this is not suitable for Monopulse Secondary Surveillance Radar (MSSR) communication which requires a large gain. Antenna arrays are generally composed of several elements of justice in the form of geometric arrangements with a certain arrangement method so that the desired radiation pattern is obtained. Viewed in terms of the size of the supply current, it can be classified as uniform and non-uniform. It is called a uniform arrangement when the current magnitude of both the magnitude and the supply phase of each element is the same. The uniform arrangement has the characteristics of a narrow main beam and a large side lobe. On the other hand, a non-uniform arrangement with a different amount of current supply for each element provides a smaller side lobe level contribution.

One of the disadvantages of microstrip antennas is the appearance of surface waves. Surface waves arise when microstrip antennas irradiate waves into the air, but there are waves trapped inside the substrate. These waves form surface waves. These waves can reduce antenna efficiency and gain, limit bandwidth, increase end-fire radiation, improve cross-polarization, and limit the working frequency range of microstrip antennas. What's more, surface waves can result in a decrease in antenna performance if not all waves are irradiated into the air.

This surface wave effect results in a decrease in antenna performance, such as VSWR, return loss, and antenna efficiency. Therefore a way is needed to suppress surface waves. One way to suppress surface waves is to use the DGS or Defected Ground Structure

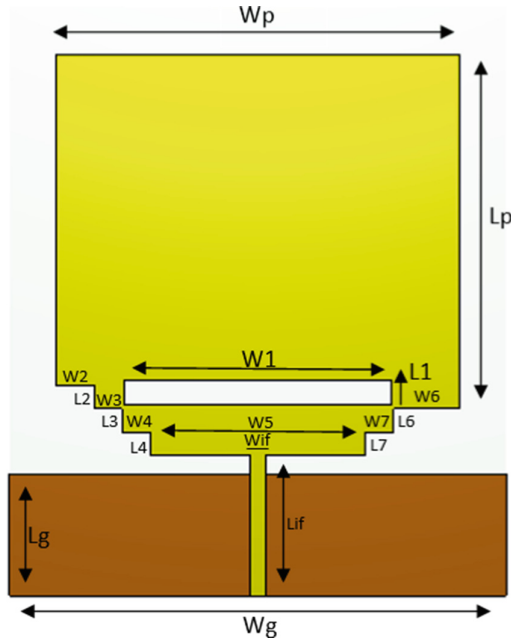


**Fig. 1.** Single microstrip antenna

(DGS) technique. The DGS technique applied in this study is by disfiguring the ground field on the microstrip antenna [11, 12].

## 2 Method

In this study using the DMS (Defected Microstrip Structure) method, this method was used to reduce or add structure to the patch antenna. In addition to using the DMS (Defected Microstrip Structure) method, this study also uses the DGS (Defected Ground Structure) method, in contrast to the first method, this time the method that was changed was not the patch but from the ground side, it can be seen in Fig. 1. In this design the material used to make the substrate is Fr-4 with a dielectric constant [13] of  $\epsilon_r = 4.3$  and the substrate thickness ( $h$ ) = 1.6 mm. And for its patch, it uses copper material with a patch thickness of 0.035 mm.

Figure 1 is a picture of a single microstrip antenna with a wideband beam with a range of 1030–1090 MHz. On the microstrip antenna, it has also used the DMS (Defected Microstrip Structure) and DGS (Defected Ground Structure) methods with sizes,  $W_p = 86\text{mm}$ ,  $L_p = 86\text{mm}$ ,  $W_1 = 57\text{mm}$ ,  $L_1 = 5\text{mm}$ ,  $W_2 = 8\text{mm}$ ,  $L_2 = 5\text{mm}$ ,  $W_3 = 6\text{mm}$ ,  $L_3 = 5\text{mm}$ ,  $W_4 = 6\text{mm}$ ,  $L_4 = 5\text{mm}$ ,  $W_5 = 46\text{mm}$ ,  $W_{if} = 3\text{mm}$ ,  $L_{if} = 30\text{mm}$ ,  $W_6 = 14\text{mm}$ ,  $L_6 = 5\text{mm}$ ,  $W_7 = 6\text{mm}$ ,  $L_7 = 5\text{mm}$ ,  $L_g = 26\text{mm}$ ,  $W_g = 106\text{mm}$ .

Figure 2 is the result of a microstrip antenna that has used the DGS (Defected Ground Structure) method and the DMS (Defected Microstrip Structure) method the results show that the microstrip antenna has become wideband and has met the expected frequency range criteria, which is between 1030 MHz–1090 MHz.

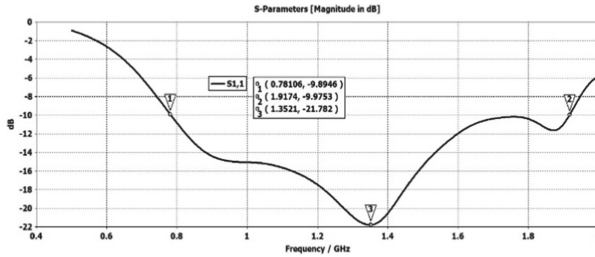


**Fig. 2.** Results of a Single microstrip antenna

**Table 1.** Wideband antenna calculation results

Kind of soil	Symbol	Specifications
Patch Length	Lp	86 mm
Patch Width	Wp	86 mm
Length of Feeding Inserts	Lif	30 mm
Width of Feeding Insert	Wif	3 mm
Substrate Length	Ls	126 mm
Substrate Width	Ws	106 mm
Patch Length 1/2 Lamda	D	140 mm
Patch Insert Width 1	W1	57 mm
Patch Insert Length	L1	5 mm

To get optimal results on antenna equipment, it is necessary to carry out several simulations and optimizations on a parameter. Here we have optimized our antenna so that we get the expected wideband, which is in the range of 1030 MHz–1090 MHz (Table 1).

### 3 Results and Discussion

In this discussion, we will see, describe and compare return loss, VSWR, gain, and angular width, compared to these parameters are very important for designing an antenna. Return Loss is one of the parameters used to find out how much power is lost on the load and not returned as a bounce. Return loss has an origin that synergizes with VSWR, which occurs due to a mixture of transmitted waves and reflected waves which both determine the matching between the transmitter device and the antenna.

VSWR is the ratio between an incoming wave and a reflective wave where the two waves form a standing wave. Standing Wave is a combination of reflection and interference, namely the reflective wave interfering with the coming wave so that the phase of the coming wave is disturbed by the reflective wave which causes the incoming

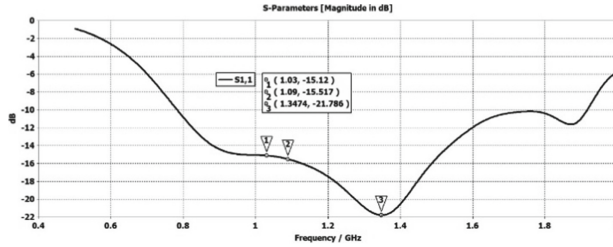


Fig. 3. Return Loss Value

wave to be damaged. The higher the VSWR value means that the performance of the antenna is not better or the wave that intervenes is greater [14–16].

Gain (directive gain) is an antenna character related to the ability of the antenna to direct its signal radiation or the reception of a signal from a certain direction. Gain is not a quantity that can be measured in physical units in general such as watts, ohms, or others, but rather a form of comparison. Therefore, the unit used for gain is decibel [17–19].

Antenna Radiation Pattern (Radiation Pattern) is a depiction of radiation related to the strength of radio waves emitted by the antenna or the level of signal reception received by the antenna at different angles. In general, this Radiation Pattern is depicted in the form of a 3-dimensional plot. This 3-dimensional antenna radiation pattern is formed by two radiation patterns, namely the elevation pattern and the azimuth pattern. The form radiation pattern is the Omnidirectional pattern, which is the same radiation pattern in one field of radiation, and the Directive Pattern which forms a narrow beam sphere with high radiation. In the discussion below, we will discuss the parameters described above [20, 21].

Gain (directive gain) is an antenna character related to the ability of the antenna to direct its signal radiation, or the reception of a signal from a certain direction [22, 23]. Gain is not a quantity that can be measured in physical units in general such as watts, ohms, or others, but rather a form of comparison. Therefore, the unit used for gain is the decibel.

### 3.1 Return Loss

Hasil the Return Loss parameter of the single antenna can be seen in Fig. 3 below. From these parameters, the frequency used on the x-axis starts from a frequency of 0.5 GHz to 2 GHz. Furthermore, on the Y axis, the magnitude return loss value starts from 0 dB to  $-22$  dB.

In Fig. 3 in the middle of the curve, there is a triangular symbol. The symbol is useful for marking the return loss value at each frequency. Symbol number 1 on the frequency of 1030 MHz shows the result of  $-15.12$  dB, symbol number 2 on the frequency of 1090 MHz shows the result of  $-15.51$  dB and which shows the best result obtained at a frequency of 1374 MHz with a return loss value of  $-21.78$ .

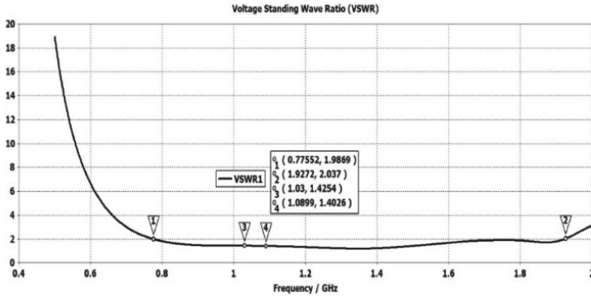


Fig. 4. VSWR Value

### 3.2 VSWR

Figure 4 shows the VSWR graph at a working frequency of 1030 MHz–1090 MHz. In the graph the frequency starts at a frequency of 0.5 GHz equals the frequency of 2 GHz then for the null graph the VSWR is shown from a value of 0 dB to 20 dB.

There is a triangular symbol in the middle of the curve used as a marker that shows the SWR value of the simulation result. The value obtained at each frequency can be seen in the first symbol at the frequency of 775 MHz getting an SWR value of 1.9 dB, then in the second symbol at the frequency of 1927 MHz getting an SWR value of 2.3, for the third symbol of the frequency of 1030 MHz getting an SWR value of 1.4 dB, and for the last symbol at a frequency of 1090 MHz get an SWR value of 1.4 dB. Judging from the results of each of these symbols, there is a correlation with the return loss value in Fig. 2. The higher the return loss value, the lower the SWR value. If  $VSWR = 1$  then the entire power will be emitted through the antenna.

### 3.3 Bandwidth

The results of the parameters of the bandwidth can be seen in Fig. 2 above. It shows the frequency value against the magnitude value of the antenna's return loss. The bandwidth value is obtained by taking a larger working frequency equal to 10 dB. The triangle symbol in Fig. 2 shows the amount of bandwidth value on the antenna. The way to calculate the bandwidth is using the upper frequency which is indicated by the symbol no. 2 with a frequency value of 1352 MHz minus the lower frequency value indicated by symbol number 1 with a frequency of 781 MHz to get a bandwidth result of 571 MHz.

### 3.4 Gain

Figure 5 below shows the gain value on the single antenna displayed in the form of a graph.

In Fig. 5, 3 triangles indicate the gain value at each frequency. In symbol number 2, the frequency of 1030 MHz gets a gain value of 2.83 dB, then symbol number 3 gets a gain value of 3.00 dB, and the highest gain value is on symbol no. 3 with a gain value of 6.37 dB.

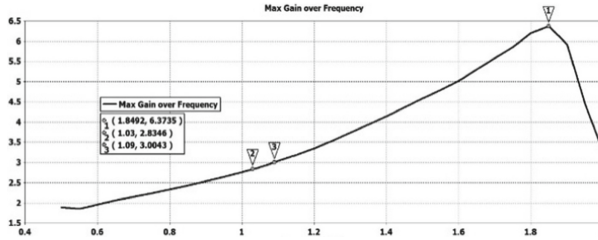


Fig. 5. Gain Antenna Value

### 3.5 Radiation Pattern

Figure 6 shows the simulation results of the radiation pattern. The image shows the main lobe magnitude, main lobe direction, angular width (3 dB), and side lobe level. The main lobe magnitude is indicated by a broken line that intersects with the main lobe direction in the middle. The inner circle shows the value of the isotropic radiation and the middle circle is a reference to the position of the circle. The sliced circle sign forming the pizza slices shows the angular width value and the centerline between the slices indicates the main lobe direction value.

The value of the radiation pattern on the antenna can be seen in Figs. 6a, and 6b. in this discussion, the angular width value at a frequency of 1030 MHz is highlighted at 173.00 and a frequency of 1090 MHz at 171.00.

### 3.6 Surface Current

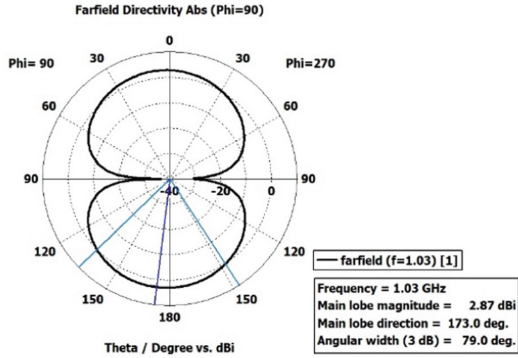
Figure 7 is the result of a surface current simulation, the current moves through the recording channel then pass through the patch and spread to the ground, the largest current is found in Most of the antenna patches, and is also on the sidelines of the insert feeding antenna, under the current distribution there is maximum current value 61 A/m.

In Fig. 7, there is only a picture of the current distribution of a single antenna. The maximum current rated of the 1030 MHz and 1090 MHz frequencies is 60 A/m. Following Kirchhoff's Law, I state that the amount of current entering a branch is equal to the amount of current out of a branching.

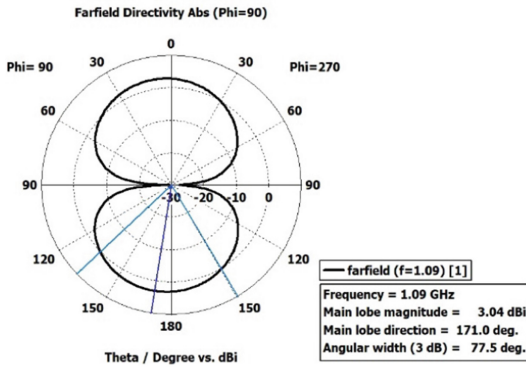
### 3.7 Axial Ratio

Figure 8 shows a graph of the Axial Ratio value at a frequency of 1030 MHz–1090 MHz. in the chart the frequency range is run starting from a frequency of 0.5 GHz–2 GHz and for the axial ratio results seen in the chart starting at a value of 35.5 dB–40 dB.

In Fig. 7 there are 4 symbols listed on the chart. Symbol number 1 at a frequency of 1030 MHz obtained the Axial ratio value of 40 dB, then in the second graph at a frequency of 1090 MHz obtained a value equal to symbol number one, namely 40 dB, then for symbol number 3 at a frequency of 1299 MHz the Axial Ratio value shows a decreasing graph at a value of 35.63 dB, and the last symbol no. 4 at a frequency of 1650 MHz the chart shows a rise again at the value of 39.1 dB. From some of these



a Radiation Pattern 1030 MHz



b Radiation Pattern 1090 MHz

Fig. 6. Radiation Pattern Value

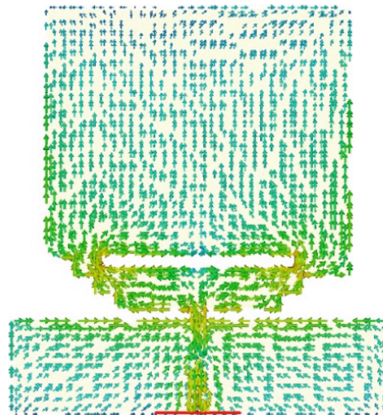
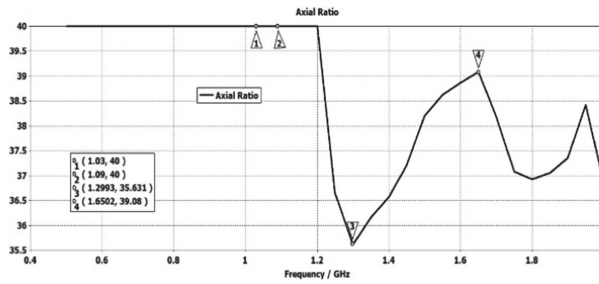


Fig. 7. Current distribution on the antenna





**Fig. 8.** Axial Ratio Value

**Table 2.** Simulation Results of wideband antenna

Antenna Parameters	1030	1090
Return Loss	-15.12	-15.51
VSWR	1.4	1.4
Bandwidth	571 MHz	
Gain	2.83 dB	6.37 dB
Angular Width	173.00	171.00,
Surface Current	61 A/m	61 A/m
Axial Ratio	40 dB	40 dB

values, it can be concluded that the Axial Ratio value on the microstrip antenna using the DGS (Defected Ground Structure) method and the DMS (Defected Microstrip Structure) method show values that are not always fixed but always changing.

## 4 Conclusion

In this research, we succeeded in designing a wideband microstrip antenna with a frequency range of 1030 MHz–1090 MHz using the DGS (Defected Ground Structure), and DMS (Defected Microstrip Structure) methods. From the simulation results and several evaluations obtained the results shown as shown in Table 2.

Table 2, it shows that the results at each frequency are not much different, there are only a few lower values and some are higher. One of them is in the gain value shown at a frequency of 1030 MHz, the value is lower when compared to the frequency of 1090 MHz.

## References

1. M. Grilo and F. Saleté Correra, "Parametric study of rectangular patch antenna using denim textile material," 2013 SBMO/IEEE MTT-S International Microwave & Optoelectronics Conference (IMOC), pp. 1–5, Aug. 2013, doi: <https://doi.org/10.1109/IMOC.2013.6646439>.

2. B.-K. Ang and B.-K. Chung, "A WIDEBAND E-SHAPED MICROSTRIP PATCH ANTENNA FOR 5 - 6 GHZ WIRELESS COMMUNICATIONS," *Progress In Electromagnetics Research*, vol. 75, pp. 397–407, 2007, doi: <https://doi.org/10.2528/PIER07061909>.
3. I. Mohd Ibrahim et al. , "Parametric Study of Modified U-shaped Split Ring Resonator Structure Dimension at Ultra-Wide-band Monopole Antenna," *Journal of Telecommunication, Electronic and Computer Engineering*, vol. 10, pp. 2–5, 2018, [Online]. Available: <https://www.researchgate.net/publication/328095758>
4. S.-L. S. Yang, A. A. Kishk, and K.-F. Lee, "Wideband Circularly Polarized Antenna With L-Shaped Slot," *IEEE Trans Antennas Propag*, vol. 56, no. 6, pp. 1780–1783, Jun. 2008, doi: <https://doi.org/10.1109/TAP.2008.923340>.
5. G. Chaitanya, A. Arora, A. Khemchandani, Y. Rawat, and S. Singhai, "Comparative study of different Feeding Techniques for Rectangular Microstrip Patch Antenna," *INTERNATIONAL JOURNAL OF INNOVATIVE RESEARCH IN ELECTRICAL, ELECTRONICS, INSTRUMENTATION AND CONTROL ENGINEERING*, vol. 3, no. 5, pp. 2321–5526, 2015, doi: DOI <https://doi.org/10.17148/IJIREEICE.2015.3509>.
6. Z. Zakaria, W. Y. Sam, M. Z. A. Abd Aziz, and M. A. Meor Said, "Rectangular microstrip patch antenna based on resonant circuit approach," in *2012 IEEE Symposium on Wireless Technology and Applications (ISWTA)*, Sep. 2012, pp. 220–223. doi: <https://doi.org/10.1109/ISWTA.2012.6373847>.
7. O. O. Strelnytskyi, I. v. Svyd, I. I. Obod, O. S. Maltsev, and G. E. Zavolodko, "Optimization of Secondary Surveillance Radar Data Processing," *International Journal of Intelligent Systems and Applications*, vol. 11, no. 5, pp. 1–8, 2019, doi: <https://doi.org/10.5815/ijisa.2019.05.01>.
8. B. B. Harianto, M. Rifa, Y. Suprpto, T. Warsito, and A. Mauludiyanto, "2x2 Array Circular Microstrip Antenna Design for Altimeter Radar Antenna Applications," pp. 54–62.
9. J. H. Choi, J. H. Jang, and J. E. Roh, "Design of an FMCW Radar Altimeter for Wide-Range and Low Measurement Error," *IEEE Trans Instrum Meas*, vol. 64, no. 12, pp. 3517–3525, 2015, doi: <https://doi.org/10.1109/TIM.2015.2450294>.
10. K. Harshasri, P. V. Babu, and P. N. Rao, "Design of Compact C-Band Concave Patch Antenna for Radar Altimeter Applications," *Proceedings of the 2018 IEEE International Conference on Communication and Signal Processing, ICCSP 2018*, pp. 542–546, 2018, doi: <https://doi.org/10.1109/ICCCSP.2018.8524261>.
11. A. Kakkar, Nirdosh, and S. Sah, "A tri-band circular patch microstrip antenna with different shapes in DGS for Ku and K applications," *2nd International Conference on Telecommunication and Networks, TEL-NET 2017*, vol. 2018-Janua, pp. 1–5, 2018, doi: <https://doi.org/10.1109/TEL-NET.2017.8343500>.
12. W. A. Awan, A. Zaidi, and A. Baghdad, "Patch antenna with improved performance using DGS for 28GHz applications," *2019 International Conference on Wireless Technologies, Embedded and Intelligent Systems, WITS 2019*, pp. 1–4, 2019, doi: <https://doi.org/10.1109/WITS.2019.8723828>.
13. A. Boutejdar, M. A. Salamin, S. D. Bennani, and S. el Hani, "Design of compact monopole antenna using double U-DMS resonators for WLAN, LTE, and WiMAX applications," *Telkomnika (Telecommunication Computing Electronics and Control)*, vol. 15, no. 4, pp. 1693–1700, Dec. 2017, doi: <https://doi.org/10.12928/TELKOMNIKA.v15i4.7666>.
14. J. R. James and P. S. Hall, *Handbook of Microstrip Antennas*, Second Edition. 1989.
15. M. Mazanek, M. Polivka, P. Cerny, P. Hazdra, P. Piksa, and P. Pechac, "Education in Antennas, Wave Propagation and Microwaves," *AUTOMATICS: časopis za automatiku, mjerenje, elektroniku, računarstvo i komunikacije*, vol. 47, no. 3–4, 2006.
16. M. Mazanek, M. Polivka, P. Cerny, P. Piksa, and P. Pechac, "Education in Antennas, Wave Propagation and Microw Ave Techniques," 2005. doi: <https://doi.org/10.1109/ICECOM.2005.205003>.

17. H. W. Lai, Fong Lee Fabric, Kwai Man Luk, Microstrip Patch Antennas, vol. 2, no. X. 2017. doi: <https://doi.org/10.1007/s13398-014-0173-7.2>.
18. D. G. Fang, Antenna Theory and Microstrip Antennas. 2011.
19. H. W. L. Kai Fong Lee, Kwai Man Luk, Microstrip Patch Antennas (Second Edition, 2nd ed. World Scientific, 2017.
20. S. Ülker, "Antennas and propagation course in education," International Journal of Electrical Engineering and Education, vol. 57, no. 4, pp. 281–300, 2020, doi: <https://doi.org/10.1177/0020720918800441>.
21. S. Ülker, "Antennas and propagation course in education," International Journal of Electrical Engineering and Education, vol. 57, no. 4, 2020, doi: <https://doi.org/10.1177/0020720918800441>.
22. W. L. Stutzman and G. A. Thiele, Antena Theory and Design. John Wiley and Sons, Inc. 2012.
23. K. F. Lee, "A personal overview of the development of microstrip patch antennas," 2016 IEEE Antennas and Propagation Society International Symposium, APSURSI 2016 - Proceedings, pp. 689–690, 2016, doi: <https://doi.org/10.1109/APS.2016.7696053>.

**Open Access** This chapter is licensed under the terms of the Creative Commons Attribution-NonCommercial 4.0 International License (<http://creativecommons.org/licenses/by-nc/4.0/>), which permits any noncommercial use, sharing, adaptation, distribution and reproduction in any medium or format, as long as you give appropriate credit to the original author(s) and the source, provide a link to the Creative Commons license and indicate if changes were made.

The images or other third party material in this chapter are included in the chapter's Creative Commons license, unless indicated otherwise in a credit line to the material. If material is not included in the chapter's Creative Commons license and your intended use is not permitted by statutory regulation or exceeds the permitted use, you will need to obtain permission directly from the copyright holder.

